Eur Biophys J (2000) 29: 134–140

BIOPHYSICS LETTER

Fabien Gerbal · Valérie Laurent · Albrecht Ott
Marie-France Carlier · Paul Chaikin · Jacques Prost

Measurement of the elasticity of the actin tail of *Listeria monocytogenes*

Received: 13 October 1999 / Revised version: 14 January 2000 / Accepted: 18 January 2000

Abstract We report biophysical experiments performed on the bacterium *Listeria monocytogenes*, a model system to study actin-based motility. Using optical tweezers and electrophoresis experiments, we find that the bacterium is firmly attached to its tail, and we demonstrate that the tail responds as an elastic gel when deformed. We have measured its elastic modulus at a value of 10^3–10^4 Pa, which is 10 times higher than the rigidity of the eukaryotic cytoplasm. These results demonstrate that the bacterium and its tail form a very robust system, consistent with the steadyness of the motion observed in vivo. We propose an elastic model for the propulsion mechanism which takes into account the connection and thus the interaction between the actin filaments. It provides a generic description of the various aspects of actin-tail based movements.

Key words *Listeria monocytogenes* · Cell motility · Actin gel · Elasticity · Optical tweezers · Cell mechanics

Introduction

Listeria monocytogenes is a pathogenic bacterium which induces actin polymerization at its surface (Tilney and Portnoy 1989; Southwick and Purich 1996). It creates a long tail of cross-linked actin gel used as a scaffolding to propel itself through the cytoplasm and the membranes of infected cells (Theriot et al. 1992). This is one of the simplest systems whose motion shares many features with eukaryotic cell motility (Friedrich et al. 1995). A detailed description of the molecular agents (Kocks et al. 1995; Welch et al. 1998) involved in its displacement has been facilitated by the reconstitution of *Listeria* motility in cell-free extract medium [cytoplasm of *Xenopus* eggs (Theriot et al. 1994) or of blood platelets (Carlier et al. 1997)] (Fig. 1). Many models suggest how the polymerization of actin monomers is biochemically achieved (Marchand et al. 1995; Southwick and Purich 1998). No ATPase proteins like myosins have been found to be involved (Dabiri et al. 1990; Mounier et al. 1990; Marchand et al. 1995), and actin polymerization alone is thought to account for the *Listeria* motion (Mitchison and Cramer 1996). Only Oster et al. have proposed a quantitative predictive model (Peskin et al. 1993; Mogilner and Oster 1996) explaining how the actin polymerization produces forces driving *Listeria* or extending lamellipodia at the leading edge of motile cells. In this paper, we present the first quantitative measurements of the elasticity of the *Listeria* actin tail. Our results provide a basis to estimate the intensity of the forces propelling the bacterium owing to actin polymerization.

F. Gerbal (✉)[1] · A. Ott · J. Prost
Institut Curie (UMR 168), 11 Rue Pierre & Marie Curie, 75231 Paris Cedex 05, France

V. Laurent · M.-F. Carlier
LEBS (UPR 9063) CNRS, 91198 Gif sur Yvette, France

P. Chaikin
Department of Physics, Jadwin Hall, Princeton University, Princeton, NJ 08544, USA

Present address:
[1]Princeton University, Princeton, NJ 08544, USA
e-mail: fgerbal@princeton.edu

Materials and methods

Sample preparation

L. monocytogenes (Lut12 pactA3 strain overexpressing ActA) stored at −80 °C were thawed, washed, and resuspended at 6×10^9 bacteria/ml in XB buffer (10 mM HEPES-KOH buffer, pH 7.7, 100 mM KCl, 1 mM $MgCl_2$, 0.1 mM $CaCl_2$, 50 mM sucrose). The bacteria suspension (1 µl) and 1 µl of a 80 mM ATP-Mg solution were added to a mix of 2 µl *Xenopus* egg extract and 18 µl human blood platelet extract. The combination of

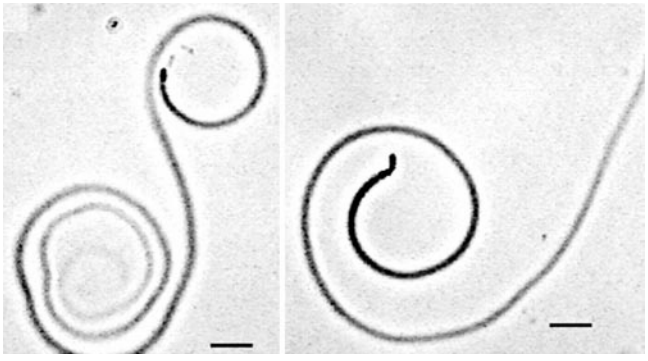

Fig. 1 Phase contrast images of *Listeria* with their tails in 90% platelets cytosol extract and 10% *Xenopus* extract. Platelets high-speed supernatants do not contain vesicles and are suitable for experiments with optical tweezers. The addition of *Xenopus* extract increases the percentage of motile bacteria. The speed increases exponentially with temperature. At 35 °C, *Listeria* moved at 9.2 ± 0.17 μm/min (18 measurements) and the depolymerization time was about 5–10 min, so that tails could be more than 100 μm long. *L. monocytogenes* can grow helix-shaped tails (here, they adhere to the surface) with a constant curvature over more than 50 μm. *Bars* are 5 μm long

the two extracts was essential to obtain very long actin tails and rapid *Listeria* movement. Then 1 μl of a suspension of 1.909 μm diameter latex beads (Polyscience) at $\sim 10^9$ beads/ml was added. Then 5 μl of this solution was placed between a slide and a coverslip coated with bovine serum albumin, the sample was sealed with superglue, and movement was observed using a phase contrast Plan-Neofluar 100X/1.3 oil objective (Zeiss) in an inverted microscope (Zeiss Axiovert 135). The temperature was set to 35 ± 0.5 °C. The images obtained from a gray level CCD Sony camera were recorded with a S-VHS videorecorder.

Optical tweezer set-up

Our tweezers (Ashkin and Dziedzic 1986) were set up as described by Svoboda and Block (1994). We used a YAG Spectra Physics laser (model 7300, $\lambda = 1064$ nm, maximum power 600 mW, mode T_{00}). The beam was first deflected by two mirrors on a galvanometer positioning system (650× from Cambridge Technology) and passed through a 2.5× beam expander before being focused through the objective. The geometry was such that an elementary angular displacement of the galvanometers moved the tweezer by 20 nm. The main beam could be split into two or three traps by controlling the mirrors with a 100 Hz square periodic function.

We calibrated the maximum force a tweezer could apply on a latex bead versus the power of the laser. The beads were dragged trough a 12% glycerol in water solution having the same refraction index as our motility medium (1.347 ± 0.001) and a known viscosity of 1.23×10^{-3} Pa s (measured in a Brookfield conic Couette viscosimeter). The frequency of a sinusoidal displacement (added to the multi-trap function) was increased until the bead was dragged out of the trap when the Stokes force ($F = 6\pi\eta RV$) equaled the optical force. For multiple trapping, we checked each trap independently and found a dispersion less than 2% induced by the variation of the laser intensity with position. The calibrated force was linear with the laser power for slow displacements (when the displacement period is long compared to the multi-trap function period). Since in our experiments the beads escaped at such a low speed from the traps, measurements at low laser power were linearly extrapolated to obtain the full calibration curve. The viscosity of the motility medium was measured by comparing the viscous drag on a bead with the optical force and found to be 0.03 ± 0.01 Pa s. The force exerted by a single trap tweezer on a bacterium was evaluated following the same protocol and found to be about 10 pN.

Optical scissors

We used a Spectra Physics argon laser (model Stabilite 2017) focused through the objective to cut *Listeria* tails. We found that 10 s of continuous illumination with 200 mW of radiation between 411 and 514 nm triggered the disintegration of the tail in 5–30 s on a scale of 1 μm or less. The cuts, even as close as 2 μm from a bacterium, did not affect the growth of the tails from the bacterium surface.

Sticking beads on the tail

We used 1.909 μm Polyscience carboxylate latex spheres on which functional myosin II purified from chicken breast muscles were covalently bound. The beads were manipulated within the *Listeria* solution under the microscope with the optical tweezer and stuck close to a tail. To avoid competition between actin filaments of the tail with free actin monomers in bulk (which leads to the release of the bead), we strongly irradiated the bead with 200 mW argon laser light at 514 nm to block the myosin in the strong binding state. After such treatment the beads remained stuck for minutes and never detached from the tail when pulled away with the tweezer, until the usual depolymerization of the tail released the bead. We were able to stick beads on the tail as close as 3 μm to a bacterium without changing its behavior.

Electrophoresis experiment

The electric field set-up used a design as described by Mitnik et al. (1995). The force was calibrated by measuring the field which would pull a free bacterium out of an optical trap (this measure takes into account the drag due to the electro-osmosis flow). The intensity of the field was limited to about 10^4 V m^{-1}, as higher field would generate too much heat in the sample.

Elastic measurements analysis

The images of the deformed tails were digitized from videotape using a Macintosh with a Scion Image Grabbers card and NIH Image software. The analysis was done on the last frame before a bead broke free of the trap, at which point the tweezers apply their maximum force and the experimental accuracy is best. To define the tail shape, 10–30 dots were plotted on the image. The fits of the theoretical shapes to the experimental tail shapes were done by the minimization of χ^2.

Results

Our first experiments involved semi-quantitative measurements of the interaction between *Listeria* and its tail. *Listeria* were studied in 6 μl of cell-free extract motility medium. In Fig. 2a and b the bacterium is held by an optical trap, and the sample cell is translated either along the tail-bacterium axis (a) or perpendicularly to it (b). This creates a viscous drag on the tail intended to pull it away from the bacterium. In both experiments the bacterium broke free of the optical trap before any separation with its tail could be seen, regardless of the length of the tail, which could be cut at various distances from the bacterium. These experiments show that the bacterium is bound to its tail by interactions stronger than 10 pN, the force exerted by the trap on a bacterium. This is about 1000 times larger than the viscous drag experienced by a moving bacterium in the extract. In another experiment (not shown), the tail is bound to a polystyrene bead attached to the cover slip. An electric field of 10^4 V m^{-1} is then applied which pulls the bacterium with a force of about 1 pN (deduced by comparison with the force of the optical tweezer) during a time scale of 2 min. This is not sufficient to pull the bacterium away from its tail (the relative displacement is less than half a micron), and there is no obvious increase in the *Listeria*'s speed. We conclude that either the filaments are temporarily bound to the bacterium, or that there is a steric hindrance to their motion (they are entangled in the bacterial wall, for instance). Thus, the experiments provide a lower boundary for an effective friction coefficient ξ between the tail and the bacterium surface: $\xi > 1$ pN/(0.5 μm/120 s) $= 2 \times 10^{-4}$ Pa m s. The connection between *Listeria* and its tail is an unexpected result as the Brownian ratchet model (Peskin et al. 1993; Mogilner and Oster 1996, 1999) suggests the filaments are only pushing on the bacterium.

In another experiment, we tried to stop the bacterium with the tweezer (Fig. 2c). We found that the tail, held by the bacterium at one tip and blocked at the other extremity by the viscous drag, bends because of the continuous actin polymerization. This increases the force from the tail on the bacterium until it is able to push the *Listeria* out of the trap. In all experiments, after the constraints are released the tails return to their original shape, showing that the deformations are elastic.

To evaluate the forces felt by the bacterium for a given strain in the tail, we performed experiments to measure the elastic modulus of the tail. We used the multiple trap optical tweezer created by deflecting the infrared laser beam with two perpendicular mirrors mounted on computer-controlled galvanometers which we oscillated between two or three positions. We stuck beads onto the tails and pulled on them until the bending forces of the tail exceeded the optical force. Depending on whether the tails were straight or curved, we used different geometries. For straight tails (Fig. 3a), we attached three beads at an equal spacing of about 10 μm (within the observation field). At first, the beam was split into three traps, catching the three beads in

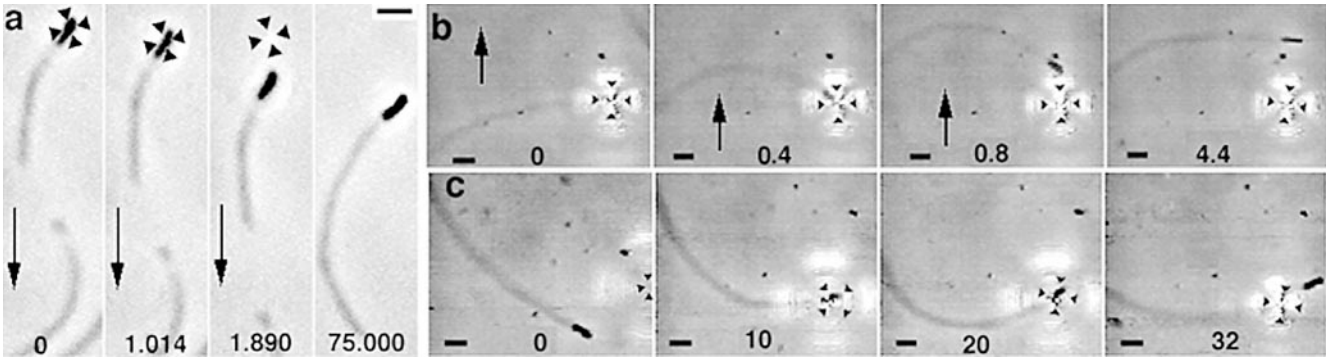

Fig. 2a–c *L. monocytogenes* is attached to its elastic tail. **a**,**b** The bacterium is held by the optical tweezer while the microscope stage is moved (the *thick arrows* indicate the direction of displacement). **a** (0 s) The tail has been cut with optical scissors, and the severed part of the tail moves away from the trapped bacterium (*1.014*). As the speed increases, the viscous force on the remaining attached tail pulls *Listeria* out of the tweezer (*1.890*). The bacterium still induces the growth of the tail after a cut by laser irradiation (*75.000*). **b** A similar experiment is performed, but with a translation perpendicular to the tail axis: a torque is exerted about the bacterium-tail contact. The angle between the bacterium and the tail does not change, but the tail bends (*0.4*). As further stress builds up with further displacement, the elastic force pushes the *Listeria* out of the trap (*0.8*). Finally, the tail recovers its initial shape (*4.4*), showing that the distortion was completely elastic. **c** A *Listeria* with a growing tail (*0*) is simply caught in the tweezer (*10*). Continued growth leads to a bending of the tail (*20*) until the elastic stress is sufficient to push the *Listeria* out of the trap. Then, the tails relaxes elastically (*32*). Tweezers are indicated by *cross-shaped markers*. *Numbers* indicate time in seconds. *Bars* = 2 μm

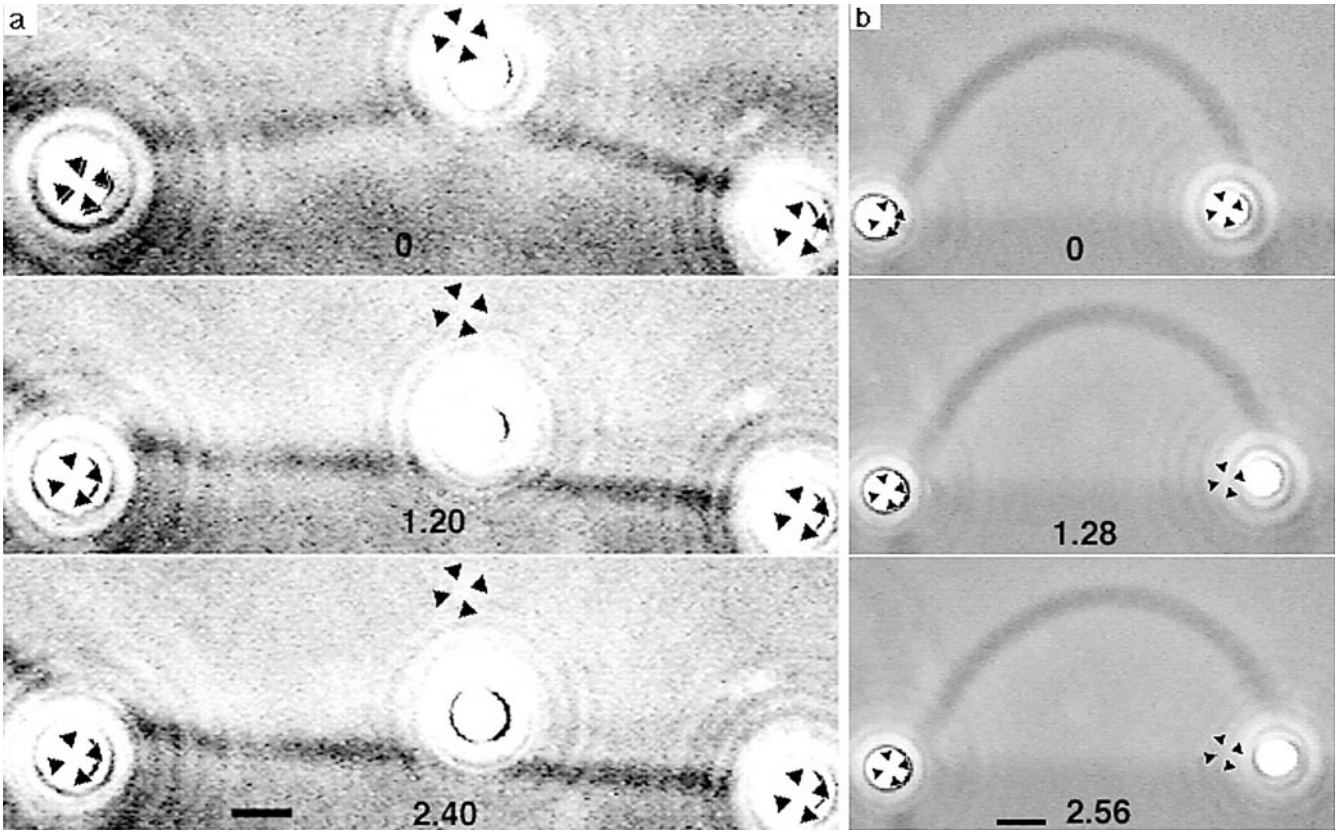

Fig. 3a, b Video images of bending experiments. Measurements of the bending modulus of straight tails (**a**) and naturally curved tails (**b**). In both sequences the first frame is the last image before a bead escapes from the tweezer, when the elastic force equals the optical force. The tails then relax to their initial equilibrium position from which they have been deformed. *Bars* are 2 μm long and times are in seconds. Tweezers are indicated by *cross-shaped markers*

their equilibrium position. We then displaced (using 20 nm steps) the central trap perpendicularly to the axis defined by the two other traps. This was done until one of the beads escaped from the trap (this was always the central bead, thus showing the dominance of bending forces over stretching; tension would have pulled out one of the side beads first). For curved tails (Fig. 3b), we attached only two beads at the extremity of a 10–30 μm long section that was then cut off from the rest of the tail using optical scissors (see Materials and methods). Then, each bead was trapped by a tweezer and one was moved in the direction of the other until one of the beads (not always the one displaced by the tweezer) escaped from its trap. The experiments were repeated an average of five times before the depolymerization of the tail caused one of the beads to detach.

The maximum force the multiple tweezers could apply on a 2 μm diameter microsphere (in the range of 1 pN) was previously calibrated by comparison with the known Stokes force due to viscous drag. The digitized images of the tail were fitted with the theoretical shape of a bent rod (Landau and Lifchitz 1967) made of isotropic and homogeneous elastic material. The average standard deviation between the fit function and the dot positions on the real tail (see Materials and methods) were found to be less than 0.1 μm for 92 of 105 measurements, indicating that the elastic model was suitable. The 13 other measurements were not included in the data since the tails did not bend homogeneously: under tension, their shape presented some kinks, suggesting that some loose parts of the gel had broken. For curved tails, left and right sides were analyzed separately to account for the natural curvature variations (~10%) and gave essentially the same rigidity. The rigidity of the tail decays with time as the actin depolymerizes (Fig. 4a). However, the tails were probed on distances (10–30 μm) such that stiffness variations due to the depolymerization could be neglected [the decay distance is typically 100 μm (Figs. 1, 4a)]. The mean value of the bending modulus K of each *Listeria* tail is plotted on Fig. 4b and ranges from 100 to 1000 $Pa(\mu m)^4$, i.e. the persistence length of the tail is in the range of a meter. This natural dispersion is directly seen by the very differing gray intensities of the phase contrast images of the tails, and is found to be the same for curved and straight tails. The log-normal distribution of the rigidity indicates that many probabilistic events are involved in the making of a tail. By comparison, the distribution of the bacterium's speed does not show such variability. Our theoretical analysis explains this result (Gerbal 1999).

No in vitro viscoelastic measurements have been performed on actin gels at concentrations higher than 50 μM. According to theoretical scaling laws (MacK-

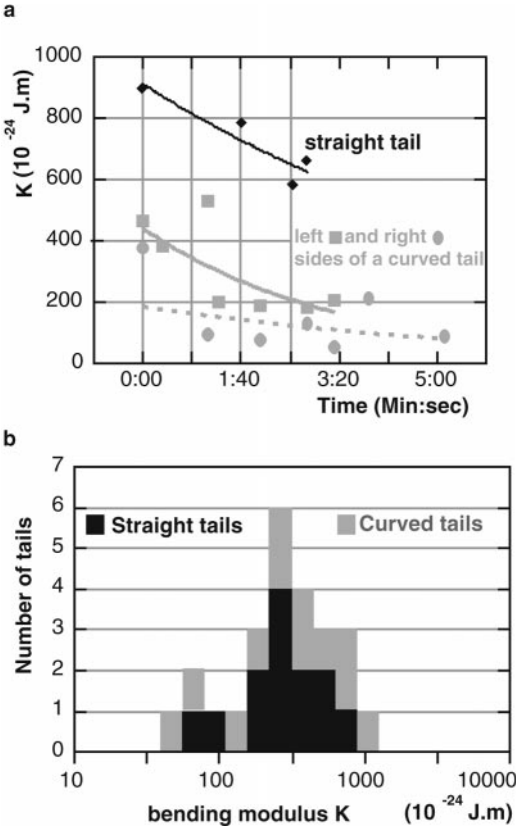

Fig. 4a, b Graphs of the bending modulus of *Listeria* tails. **a** Bending modulus (K) of two *Listeria* tails versus time (t); one straight tail (◆) and one curved tail [*gray dots* represent its left (●) and right (■) sides]. Each set of data is fitted to $A\exp(-\text{time}/\tau)$ (*continuous* and *dashed lines*), giving decay times $\tau \sim 7$, 6, 3 min, respectively, consistent with the depolymerization time of tails. **b** Distribution on a log scale of *Listeria*'s tail-bending modulus (K). *Clear bars* represent six curved tails (left and right sides) and *dark bars* represent 13 straight tails

intosh et al. 1995), an estimate of the elastic moduli of isotropic actin gels is: $G' \sim c^{2.2} \sim 10^5$ Pa, where c is the concentration found in the *Listeria* tail [in the millimolar range from freeze fracture micrographs (Sechi et al. 1997)]. This gives a rigidity of $K_{\text{big}} = G'(\pi/4)r^4 \sim 10^5$ Pa(μm)^4, where $r \sim 0.5$ μm is the radius of the tail. In the extreme alternative view, the tail is made of bundles of axial filaments able to glide on each other; this leads to a rigidity $K_{\text{small}} = nK_{\text{f}} \sim 15$ Pa(μm)^4 where $K_{\text{f}} \sim 6 \times 10^{-2}$ Pa(μm)^4 is the bending modulus of a single filament (Riveline et al. 1997) and $n \sim 200$ is the number of filaments per tail section. Our measure of K falls right between these values, suggesting either that the cross-links are not very rigid or that the tail is not homogeneous, in agreement with Sechi et al. (1997) and Zhukarev et al. (1995). Moreover, our measured values of Young's modulus of $E = K/(\pi/4)r^4 = 10^3$–10^4 Pa are consistent with recent experiments (Thoumine and Ott 1997) which showed that living chick fibroblasts have an elastic response to deformation in the range of 600–1000 Pa. It is reasonable that *Listeria* assembles a tail which is about 10 times stronger than the cytoskeleton through which it needs to move. Our measure of K implies that the tail must be entangled in the cytoplasm of an infected cell to be able to push on its membrane. The bacterium requires about 50 pN to deform a eukaryotic membrane (Evans and Yeung 1989). Such a force would buckle a long tail (as in Fig. 2c). It must be held straight by the host cytoskeleton over a distance $(\pi/2)\sqrt{(K/F_{\text{applied}})} \simeq 5$ μm (Landau and Lifchitz 1967).

Discussion

The quantitative experimental demonstration that the tail is a genuine gel firmly attached to the bacterium is not a simple confirmation of an already well-known feature. It implies that some filaments might be pulling at the same time as others are pushing on the bacterium surface, though all are connected in the gel. This shows that the interactions between the filaments are playing an important role in the propulsion of the bacterium. Thus, the *Listeria* motion cannot be deduced directly from the understanding of the biochemistry of an elementary protein set: a further analysis considering the collective behavior of the many proteins involved is also required. In the following we present a mesoscopic model of the *Listeria*, treating the gel as a continuous elastic medium (Fig. 5). Using the measurement of the tail elasticity, it provides directly an estimate of the forces driving the *Listeria*. A complete analysis of this model will be presented elsewhere (article in preparation).

Consider the growth of an actin gel from the surface of a sphere. As new gel pushes old gel outward, the outer regions stretch and exert a compressive stress inward. As the gel grows, the force on the inner surface increases until actin polymerization is no longer energetically favorable. Precisely this cessation of growth has recently been observed in vitro for actin polymerization on beads (Cameron et al. 1999; Gerbal et al. 1999) and also for some *Listeria* mutants (Lasa et al. 1997). In the case of the wild-type *Listeria*, the elastic tension is sufficiently released as the gel moves from the curved surface to the linear tail. In this model, the least energetic configuration of the gel accounts for the tail shape and the bacterium motion.

In our model, the external part of the gel (light gray on Fig. 5) and the internal part (dark gray) are treated independently at first before dealing with the full system. Consider a bacterium producing only an "external" gel by actin polymerization on its cylindrical surface [confocal microscopy observations showed that the *Shigella flexneri* tail is hollow (P. Cossart, personal communication); also Merrifield et al. have found the same result for internal vesicles propelled by an actin tail (unpublished data)]. The outward growth produces a normal stress on the bacterium side $\sigma \sim E(\delta/r)^2$ (where E is the tail Young's modulus, δ the gel thickness, and r the bacterium radius). As the gel slips off the back, it pushes the bacterium with an elastic force $F \sim E\delta^3/r$. From our

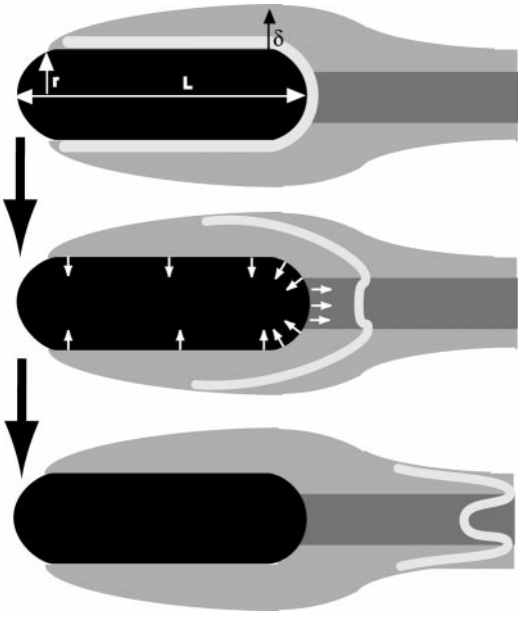

Fig. 5 Elastic model for force transduction in *L. monocytogenes*. The free energy from actin polymerization is stored as elastic energy in the actin gel, seen as a continuous medium. The shape of the tail (*dark and clear gray*) is dictated by the minimum energy conformation. The three figures describe the putative evolution of a new actin layer (*white*) polymerized on the surface at a given time. The evolution of the gel from a quasi-cylindrical geometry (around the bacterium) to a one-dimensional one (in the tail far away) induces strong deformations in the gel, thus inducing antagonist forces on the *Listeria* surface (*white arrows*). This example suggests that the external gel (*light gray*) moves faster than the internal gel (*dark gray*), so that they are respectively producing the propulsive and retarding forces

measured value of E, F is in the range of 1 nN. This propulsive force is several orders of magnitude larger than the largest external force acting on a bacterium infecting a cell (about 50 pN), or than the force required to propel a bacterium through our extract (10^{-15} N!) (see Materials and methods). The driving force F must therefore be balanced internally. Consistent with our finding that the tail and the bacterium are linked, the opposing force must be provided either by the surface friction of the gel on the bacterium, or by a tension imposed by the "internal" part of the gel produced at the back hemisphere. The strength of these forces relative to what is required for propulsion provides the steady speed of the bacteria observed in vivo: if the bacterium encounters obstacles such as cell membranes, a small compression of the elastic tail supplies the required amount of propulsive force. It is a self-adjustable mechanism. Together with the demonstrations of the attachment of the bacterium to its "engine", it shows that the tail-*Listeria* system is very robust, a requirement for infecting and moving through the eukaryote cytoplasm.

In this article, we have demonstrated the tail of *Listeria monocytogenes* is elastic. The measured value of 10^3–10^4 Pa for the Young's modulus – higher than what could be accounted for by the bending of independent filaments – is a direct demonstration that the tail is a cohesive gel, as was previously suggested by the finding of cross-linking proteins in it (Dabiri et al. 1990). These experiments provide pieces of evidence that the elasticity of the tail plays a key role in the physics of the motion: the free energy produced by the actin polymerization is used to deform the actin gel as a first step rather than producing directly the propulsive force. We propose an elastic model of the propulsion showing that the tail exerts a complex stress whose direction and strength vary along the bacterium surface, a result that cannot be obtained from a description of independent actin filaments at a molecular scale. We are able to show in a more detailed analysis (Gerbal 1999; article in preparation) that a generic actin-tail propulsion mechanism can be obtained within this elastic model, including the oscillatory behavior observed in the $ActA_{\Delta 21-97}$ mutant (Lasa et al. 1997) which periodically alternates between a fast and a slow motion.

Acknowledgements We wish to acknowledge Dominique Pantaloni for lending us his laser, and Patricia Bassereau, Pascale Cossart, Jean-Baptiste Manneville, and Dominique Pantaloni for stimulating discussions. Olivier Cardoso was of great help with his encouragement and in solving software problems.

References

Ashkin A, Dziedzic J (1986) Optical trapping and manipulation of viruses and bacteria. Science 235: 1517–1520

Cameron L, Footer M, Oudenaarden A, Theriot J (1999) Motility of ActA protein-coated microspheres driven by actin polymerization. Proc Natl Acad Sci USA 96: 4908–4913

Carlier MF, Laurent V, Santolini J, Melki R, Didry D, Xia GX, Hong Y, Chua NH, Pantaloni D (1997) Actin depolymerizing factor (ADF/cofilin) enhances the rate of filament turnover: implication in actin-based motility. J Cell Biol 136: 1307–1322

Dabiri GA, Sanger JM, Portnoy DA, Southwick FS (1990) *Listeria monocytogenes* moves rapidly through the host-cell cytoplasm by inducing directional actin assembly. Proc Natl Acad Sci USA 87: 6068–6072

Evans E, Yeung A (1989) Apparent viscosity and cortical tension of blood granulocytes determined by micropipet aspiration. Biophys J 56: 151–160

Friederich E, Gouin E, Hellio R, Kocks C, Cossart P, Louvard D (1995) Targeting of *Listeria monocytogenes* ActA protein to the plasma membrane as a tool to dissect both actin-based cell morphogenesis and ActA function. EMBO J 14: 2731–2744

Gerbal F (1999) Etude physique du mouvement de la bacterie *Listeria monocytogenes*. Thesis of university, Paris 7

Gerbal F, Noireaux V, Sykes C, Julicher F, Chaikin P, Ott A, Prost J, Golsteyn RM, Friedrich E, Louvard D, Laurent V, Carlier MF (1999) On the '*Listeria*' propulsion mechanism. Pramana 53: 155–170

Kocks C, Gouin E, Tabouret M, Berche P, Ohayon H, Cossart P (1992) *L. monocytogenes*-induced actin assembly requires the *actA* gene product, a surface protein. Cell 68: 521–531

Landau L, Lifchitz E (1967) Théorie de l'élasticité. Mir, Moscow

Lasa I, Gouin E, Goethals M, Vancompernolle K, David V, Vandekerckhove J, Cossart P (1997) Identification of two regions in the N-terminal domain of ActA involved in the actin comet tail formation by *Listeria monocytogenes*. EMBO J 16: 1531–1540

MacKintosh FC, Kas J, Janmey PA (1995) Elasticity of semiflexible biopolymer networks. Phys Rev Lett 75: 4425–4428

Marchand JB, Moreau P, Paoletti A, Cossart P, Carlier MF, Pantaloni D (1995) Actin-based movement of *Listeria monocytogenes*: actin assembly results from the local maintenance of uncapped filament barbed ends at the bacterium surface. J Cell Biol 130: 331–343

Mitchison TJ, Cramer LP (1996) Actin-based cell motility and cell locomotion. Cell 84: 371–379

Mitnik L, Heller C, Prost J, Viovy J (1995) Segregation in DNA solutions induced by electric fields. Science 267: 219–222

Mogilner A, Oster G (1996) Cell motility driven by actin polymerization. Biophys J 71: 3030–3045

Mogilner A, Oster G (1999) The polymerization ratchet model explains the force-velocity relation for growing mirotubules. Eur Biophys J 28: 235–242

Mounier J, Rytr A, Coquis-Rondon M, Sansonetti P (1990) Intracellular and cell-to-cell spread of *Listeria monocytogenes* involves interaction with F-actin in the enterocyte-like cell. Infect Immun 58: 1048–1058

Peskin CS, Odell GM, Oster GF (1993) Cellular motions and thermal fluctuations: the Brownian ratchet. Biophys J 65: 316–324

Riveline D, Wiggins CH, Goldstein RE, Ott A (1997) Elastohydrodynamic study of actin filaments using fluorescence microscopy. Phys Rev E 56: R1130–R1133

Sechi AS, Wehland J, Small JV (1997) The isolated comet tail pseudopodium of *Listeria monocytogenes*: a tail of two actin filament populations, long and axial and short and random. J Cell Biol 137: 155–167

Southwick FS, Purich DL (1996) Intracellular pathogenesis of listeriosis. New Engl J Med 334: 770–776

Southwick F, Purich D (1998) *Listeria* and *Shigella* actin-based motility in host cells. Trans Am Clin Climatol Assoc 109: 160–172

Svodoba K, Block SM (1994) Biological applications of optical forces. Annu Rev Biophys Biomol Struct 23: 247–285

Theriot JA, Mitchison TJ, Tilney LG, Portnoy DA (1992) The rate of actin-based motility of intracellular *Listeria monocytogenes* equals the rate of actin polymerization. Nature 357: 257–260

Theriot JA, Rosenblatt J, Portnoy DA, Goldschmidt-Clermont PJ, Mitchison TJ (1994) Involvement of profilin in the actin-based motility of *L. monocytogenes* in cells and in cell-free extracts. Cell 76: 505–517

Thoumine O, Ott A (1997) Time scale dependent viscoelastic and contractile regimes in fibroblasts probed by microplate manipulation. J Cell Sci 110: 2109–2116

Tilney LG, Portnoy DA (1989) Actin filaments and the growth, movement and spread of the intracellular bacterial parasite, *Listeria monocytogenes*. J Biol Chem 109: 1597–1608

Welch M, Rosenblatt J, Skoble J, Portnoy D, Mitchison T (1998) Interaction of human Arp2/3 complex and the *Listeria monocytogenes* ActA protein in actin filament nucleation. Science 281: 105–118

Zhukarev V, Ashton F, Sanger J, Sanger J, Shuman H (1995) Organization and structure of actin filament bundles in *Listeria*-infected cells. Cell Motil Cytoskeleton 30: 229–246